13P-21

Nearly chirp-free and pedestal-free pulse compression

Qian Li,[1] P. K. A. Wai,[1] K. Nakkeeran,[2] and K. Senthilnathan[1]
[1]*Photonics Research Center and Department of Electronic and Information Engineering, The Hong Kong Polytechnic University, Hong Kong.*
[2]*Department of Engineering, Fraser Noble Building, King's college, University of Aberdeen, Aberdeen AB24 3UE, UK.*

Abstract: We proposed a compact pulse compression scheme, which consists of a linear grating and a nonlinear grating, to effectively compress both hyperbolic secant and Gaussian shaped pulse profiles.

1. Introduction

Recently, we reported that pedestal-free compression of optical pulse is possible using a nonlinear fiber Bragg grating (NFBG) with exponentially decreasing dispersion profile. The input pulse however must have a hyperbolic secant pulse shape and a quadratic chirp [1]. In general, it is not easy to produce the precise pulse shape and chirp [2]. In this paper, we study the compression of initially chirp-free pulse using a linear chirped fiber Bragg grating (CFBG) to produce the required chirp profile for the compression in a NFBG with exponentially decreasing dispersion. In particular, we assume that the input pulse is a chirp-free Gaussian pulse or hyperbolic secant pulse. Our simulation results show that the pedestal generated from an input Gaussian pulse is much small than that of an input hyperbolic secant pulse showing that the compression by the NFBG is more sensitive to the chirp profile than the pulse shape. We also found that the initial Gaussian profile evolves into a hyperbolic secant profile after the compression in the NFBG.

2. Self-similar pulse compression

Self-similar pulse compression near photonic bandgap of gratings has been described in [1], where the pulse width $T(z) = T_0 \exp(-2\alpha_{20}\beta_{20}z)$ and the normalized chirp $C(z) = \alpha_{20}T_0^2 \exp(-2\alpha_{20}\beta_{20}z)$. As the normalized chirp decreases, the time-bandwidth product tends to 0.315 (transform-limited hyperbolic secant pulse). Fig. 1 shows the variation of the time-bandwidth product from 0.761 to 0.327.

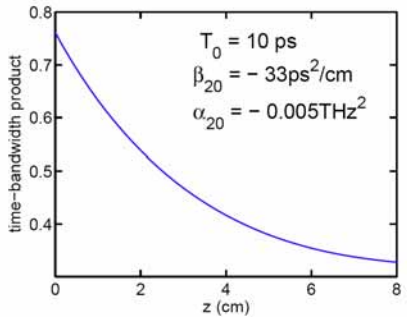

Fig.1. Evolution of time-bandwidth product.

3. Pre-chirp

First, we launched a chirp free hyperbolic secant pulse (sech(T/T_0), T_0 = 10 ps) into the linear CFBG which is 4 cm long with normal dispersion β_2 = 10 ps^2/cm. Normal dispersive medium is used here to introduce negative α_{20} required for the nonlinear pulse compression later. Fig. 2 shows the pulse profile before and after the linear CFBG in linear and logarithmic scale. From Fig. 2(d), the chirped pulse retains its hyperbolic secant pulse profile. Fig. 3 shows a polynomial fit of the phase of the pulse after linear grating CFBG. The coefficients of the t^4, t^2 and t^0 terms are 0.0111, –0.18555 and 0.168 respectively where $t = T/T_0$.

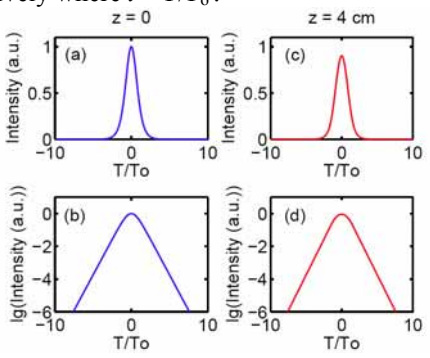

Fig.2. Pulse profile of the initial ((a) and (b)) and chirped pulse ((c) & (d)) in both linear ((a) and (c)) and logarithmic scale ((b) and (d)).

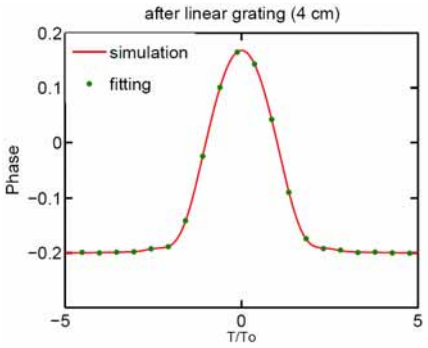

Fig.3. The phase profile after the linear CFBG.

We then launched a chirp-free Gaussian pulse (exp($-T^2/T_0^2/2$), T_0 = 10 ps) into linear grating. It is well known that the pulse after the linear CFBG is still Gaussian pulse with quadratic chirp. The chirp parameter α_{20} is chosen to be negative,

$$\alpha_{20} = -\beta_2 z / 2/(T_0^4 + \beta_2^2 z^2) < 0 \quad (1)$$

Obviously, $|\alpha_{20}| = 1/2/(T_0^4/\beta_2 z + \beta_2 z) \le 1/4T_0^2$ (2)

We choose a 4 cm long linear grating with constant dispersion β_2 = 25 ps^2/cm here for demonstration.

4. Nonlinear compression

First, we launched the chirped pulse in Fig. 2 into the NFBG. Based on the polynomial fitting result in Fig. 3,

α_{20} is set to –0.0018555 THz^2. We set $T_0^2/|\beta_{20}|=1/\gamma_g/P_0$ and choose $\beta_{20}=-40$ps^2/cm for illustration. Fig. 4 shows the pulse profile after the NFBG in both linear and logarithmic scales. The fitted hyperbolic profile (dashed lines) is of the same peak power and FWHM as final compressed pulse. We found that the pedestal energy of the final compressed pulse is 5.44% [3]. Polynomial fitting of the phase of the pulse after nonlinear grating gives the coefficients of the t^4, t^2 and t^0 terms to be 0.0041, 0.0033 and 0.5661 respectively. Compared to the results in Fig. 3, the coefficients of t^4 and t^2 are greatly reduced, i.e. the final compressed pulse is close to chirp-free. Fig. 5 shows the evolution of the FWHM of an initial hyperbolic secant pulse in the linear CFBG and the NFBG. The final FWHM compression factor (compared to initial chirp-free pulse) is 7.23.

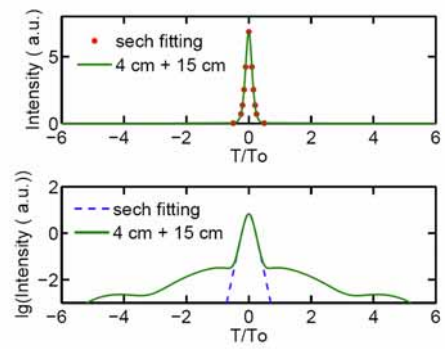

Fig.4. The final compressed pulse profile (solid lines) and the "fitted" hyperbolic secant profile (dots and dashed lines) in linear and logarithmic scales.

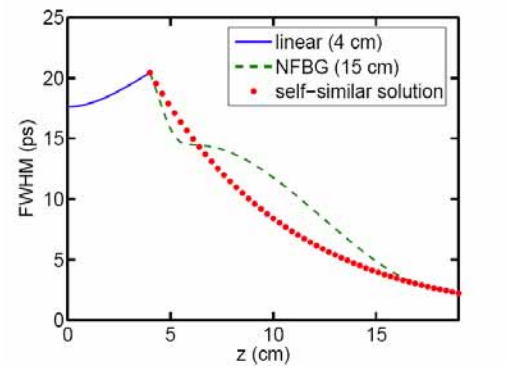

Fig.5. Evolution of the FWHM in the linear CFBG and NFBG.

Next we launched the chirped Gaussian pulse into the NFBG. Following [4] we choose the parameters

$$T^2(4\text{ cm})/\sqrt{2}/|\beta_{20}|=1/\gamma_g/P(4\text{ cm}) \quad (5)$$

where T(4cm) and P(4 cm) are the pulse width and peak power of the pulse after linear CFBG, and β_{20} is the initial dispersion value of NFBG. In our example, $\beta_{20}=-25$ ps^2/cm, T(4cm) = $10\sqrt{2}$ ps, and the NFBG is 16 cm long. Fig. 6 shows the pulse profile after the linear CFBG and after the CFBG in linear and logarithmic scales. From Fig. 6 (d), the main portion of the compressed pulse is almost the same as the fitted hyperbolic pulse. We found that the pedestal energy of the final compressed pulse is only 0.0935%. Polynomial fitting for the phase of the final compressed pulse gives the coefficients of the t^4, t^2 and t^0 terms to be –0.0007, –0.0487, –0.9355, respectively indicating that the pulse is close to transform-limited. Fig. 7 shows the evolution of the FWHM in the linear CFBG and the NFBG. The final FWHM compression factor (compared to the FWHM of initial chirp free Gaussian pulse) is 6.3.

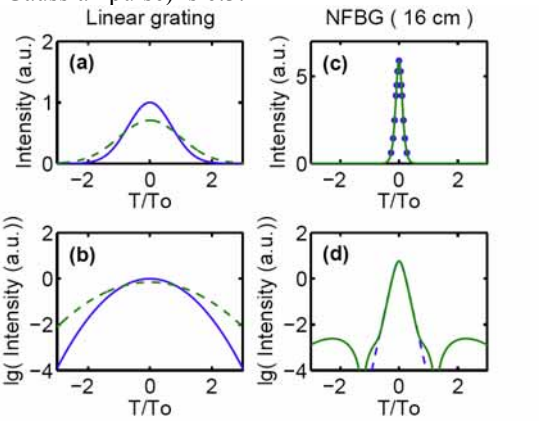

Fig.6. For a initially Gaussian pulse, the pulse profile before (solid lines) and after the linear CFBG (dashed lines) in linear scale (a) and logarithmic (b) scales). The pulse profile after the NFBG (solid lines) and the "fitted" hyperbolic secant profile (dots and dashed lines) in linear (c) and logarithmic (d) scales.

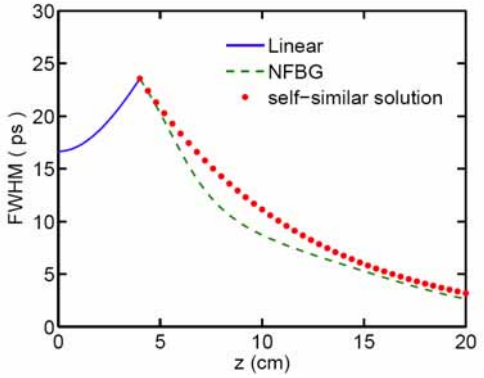

Fig.7. Evolution of the FWHM in the linear CFBG and NFBG.

5. Conclusions

We have numerically demonstrated nearly chirp-free and pedestal-free optical pulse compression using a linearly chirped fiber Bragg grating and a nonlinear fiber Bragg grating with exponentially decreasing dispersion. A compact pulse compression schemes using fiber Bragg gratings is feasible.

6. References

[1]K.Senthilnathan, P. K. A. Wai and K.Nakkeeran, Proceedings of Optical Fiber Communication, JWA 19 (1-3) (2007)

[2]D.Grischkowsky and A.C.Balant, Appl. Phys. Lett., Vol. 41, pp. 1-3, (1982)

[3]Wen-hua Cao and P. K. A.Wai, Applied Optics, Vol. 44, pp. 7611-7620, (2005).

[4]P. K. A.Wai and K.Nakkeeran, Phys. Lett. A, Vol. 332, pp. 239-243 (2004)